pp 131–147. © Royal Aeronautical Society 2017
doi: 10.1017/aer.2017.114

Control of a supersonic elliptical jet

A. Bajpai and E. Rathakrishnan
erath@iitk.ac.in
Indian Institute of Technology
Kanpur
India

ABSTRACT

Mach 2 jet from a convergent-divergent elliptical nozzle, of aspect ratio 2, has been controlled with limiting flat and arc tabs. The mixing promoting capability of the flat and arc tabs were studied in the presence of different levels of pressure gradient, at the nozzle exit, corresponding to nozzle pressure ratios of 4 to 8, in steps of one. The geometrical blockage of both the tabs is 5% of nozzle exit area. For the flat tab along the minor axis, the waves in the core become weaker and the core length becomes shorter than the uncontrolled jet, at all the NPRs studied. But the flat tab along the major axis promotes mixing only for some NPRs and retards the mixing for the rest of the NPRs studied. At NPR 5, the flat tab along the minor axis causes the largest core length reduction of 86%. For circular arc tab, along the minor axis, the maximum core length reduction is 55% at NPR 6. Arc tab along the major axis protects the core length for the entire range of the nozzle pressure ratios tested and maximum extension in core length is found at NPR 4, which is 40%.

Keywords: Jet; Supersonic; Elliptic Nozzle; Limiting Tab

Received 8 March 2017; revised 29 September 2017; accepted 3 October 2017; first published online 8 November 2017.

https://doi.org/10.1017/aer.2017.114 Published online by Cambridge University Press

NOMENCLATURE

D	equivalent diameter of the nozzle exit
NPR	Nozzle Pressure Ratio
P_t	pitot pressure
P_0	settling chamber pressure
P_e	exit pressure
P_b	backpressure
P_a	ambient pressure
X	coordinate along the jet axis
Y	coordinate along the minor axis
Z	coordinate along the major axis

1.0 INTRODUCTION

The jets have diverse nature of applicability from household application to rocket science. Control of jets is beneficial both from aerodynamics and aero-acoustic points of view. Jet controls are broadly classified into active and passive. Among them passive control is more attractive than active control, because it does not use any external power source. It is also well established that the passive control in the form of a tab enhances the mixing more efficiently than other types of passive or active control. Tab is a small solid strip kept normal to the flow with the aim of generating mixing promoting vortices. The size of the vortices shed from the tab play a dominant role in promoting the jet mixing, both in the near and far field. In addition to the tab, the geometry of the nozzle exit at which the tab is placed plays an important role in dictating the aerodynamic mixing of the jet issuing from the nozzle. For instance, the mixing enjoyed by a jet issuing from an elliptical nozzle is superior to an identical jet issuing from a circular nozzle, because of the built-in azimuthal asymmetry of the elliptical geometry. Owing to this geometrical advantage, study of jets from elliptical nozzles has become an active research area[1–4].

Bradbury and Khadem[5] were the first to study the effects of tab in low-speed jets. They observed that placement of two tabs at the nozzle exit results in the faster decay of the centerline velocity of the jet. They also reported that two tabs placed diametrically opposite at the nozzle exit is more efficient than placing more than two tabs. Samimy, Zaman and Reeder[6] reported that tabs distort the jet cross-section leading to significant increase in the jet spread. They identified that the variation of tab length for a given width did not seem to make much difference as long as the length was larger than the boundary-layer thickness. Contrary to this, Rathakrishnan[7] found that the limit for the tab length is nozzle radius and not the boundary-layer thickness. This limiting length for tab is popularly known as the *Rathakrishnan limit*. Specific investigations with a limiting tab, for three Mach numbers 1.6, 1.8, 2.0, were studied by Rathakrishnan and found that the limiting tab is efficient in promoting the jet mixing even in presence of adverse pressure gradient and becomes most efficient at the correct expansion. Arun Kumar and Rathakrishnan[8] carried out an experimental investigation to study truncated triangular tabs with corrugations in enhancing the mixing of Mach 2 circular jet, at different levels of expansion. The performance of all tabs is found to be effective in the near field at all levels of expansions. They reported 91% reduction in core length for the case of tabs with semi-circular corrugations.

Ahuja[9] investigated the effect of tabs for a circular jet with a cylindrical ejector surrounding the jet. In a study by Arun Kumar and Rathakrishnan[10], mixing promoting capability of

https://doi.org/10.1017/aer.2017.114 Published online by Cambridge University Press

a right-angled triangular tab with sharp and truncated vertex has been investigated by placing two identical tabs at the exit of Mach 2 axisymmetric nozzle. They reported that mixing caused by the right-angled triangular tab with truncated vertex is superior to the identical tab with sharp vertex and rectangular tab of equivalent blockage. They also found that the mixing promoting efficiency of tab is increased with increase in nozzle pressure ratio.

The generation mechanism of the streamwise vortex pairs by tabs and their effect on the entrainment and spreading of free jets have been investigated by Bohl and Foss[11]. Ahuja and Brown[12] reported that, for a circular jet of Mach number 1.12 and total temperature of 664 K, the potential core length could be reduced from six diameters to two diameters by using two diametrically opposed rectangular tabs. They also found considerable decrease in temperature along the jet centreline.

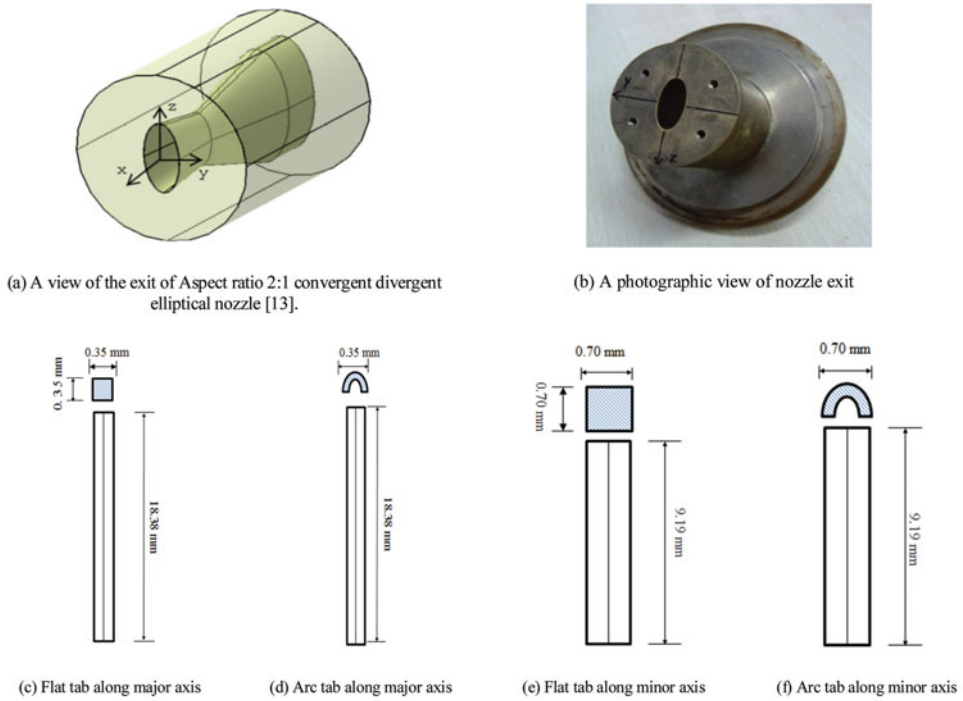
So far, limited work has been reported in literature on the control of supersonic jet with limiting tabs. Also, the reported literature is for circular jets only. Therefore, studying the control effectiveness of limiting tabs for a jet of different geometry, such as an elliptical jet, which possesses built-in geometrical advantage of azimuthal asymmetry, which enables the nozzle to shed azimuthal vortices of continuously varying size, from one end of the major axis to the adjacent end of the minor axis, in accordance with the vortex theory; that a vortex shed from an edge is proportional to the radius of curvature of the edge[13] will be of value. A mixed size of momentum transporting small-scale vortices is an advantage from aerodynamic mixing point of view; since the mixing promotion caused by the small-scale vortices of continuously varying size, such as the azimuthal vortices that shed from one quarter of the nozzle exit, would be better than that by a set of small-scale vortices of uniform size. In addition to the built-in geometrical advantage of the nozzle shape, the vortices shed from the edges of the tab would be of further advantage from aerodynamic mixing enhancement point of view. Thus, a study analysing the mixing of an elliptic jet controlled with limiting tab, capable of shedding mixing promoting vortices right up to the jet centreline, in the presence of different levels of pressure gradient will be of immense value to the field of jet research. With this aim, mixing of a Mach 2 elliptical jet issuing from a convergent-divergent elliptical nozzle, controlled with flat and arc limiting tabs located along the minor and major axes of the nozzle exit, in the presence of expansion levels corresponding to nozzle pressure ratios from 4 to 8 has been investigated in the present study. To assess the mixing promoting capability of the elliptical jet in the presence of limiting tabs, the pitot pressure decay (CPD) along the jet centerline was measured up to 20D, at 1-mm intervals, where D is the equivalent diameter–defined as the diameter of an axisymmetric nozzle having the same cross-sectional area as the elliptical nozzle exit has been studied in this work. The centreline pressure was measured at nozzle pressure ratios (NPRs) of 4, 5, 6, 7, and 8. In addition to the centreline decay, the pressure distribution along the major (Z-direction) and minor (Y-direction) axes of the jet, at different axial locations (X/D) were also measured. The waves prevailing in the jet have been visualised by the shadowgraph technique. The present results have been compared with an equivalent Mach 2 uncontrolled elliptical jet[13].

2.0 EXPERIMENTAL DETAILS

2.1 Jet test facility

The experiments were conducted in the open jet facility at the high-speed aerodynamics laboratory, Indian Institute of Technology Kanpur, India. The compressed air to the settling chamber was supplied continuously from the storage tank through a control valve. To reduce

https://doi.org/10.1017/aer.2017.114 Published online by Cambridge University Press



(a) A view of the exit of Aspect ratio 2:1 convergent divergent elliptical nozzle [13].

(b) A photographic view of nozzle exit

(c) Flat tab along major axis

(d) Arc tab along major axis

(e) Flat tab along minor axis

(f) Arc tab along minor axis

Figure 1. (Colour online) Elliptic nozzle and tabs used.

the flow disturbance caused by the control valve, a mixing length of 2 m was placed between the valve and the settling chamber. Two wire-mesh screens placed within the settling chamber condition the flow, before entering the nozzle. The desired Nozzle Pressure Ratio (NPR) was achieved by controlling the settling chamber pressure, with a pressure-regulating valve. The backpressure was the atmospheric pressure into which the jet was discharging.

2.2 Experimental model

The experimental model used in the present investigation is a Mach 2.0 convergent-divergent elliptical nozzle of 2:1 aspect ratio, made of brass. The equivalent throat and exit diameters of the nozzle are 10 mm and 13 mm, respectively. The Reynolds numbers of the Mach 2.0 jet, based on nozzle exit diameter are 7.12×10^5 and 16.6×10^5, respectively, for the NPRs 4 and 8. Some views of the elliptical nozzle exit (with and without tab) are shown in Fig. 1. The tabs used were of flat and circular-arc geometries. The flat tab placed along the major axis is of width 1.45 mm and length 18.38 mm, and the flat tab along the minor axis is 2.88 mm in width and 9.19 mm in length. The limiting arc-tab along the major axis is of width 1.45 mm and length 18.38 mm and the limiting arc-tab along the minor axis is of length 9.19 mm and width 2.88 mm. For both tabs, the blockage ratio (projected area of the tab normal to the flow direction/nozzle exit area) is 5%. The flat tab is made of brass and the arc tab is made from a hypodermic needle. The geometrical dimensions of the tab are given in Fig. 1. A face of the square tab was kept normal to the jet axis for both tabs along the major and minor axes. Similarly, the convex face of the circular arc tab was kept normal to the jet axis for both the orientations; along the major and minor axes. Because of the flat face of the square tab

https://doi.org/10.1017/aer.2017.114 Published online by Cambridge University Press

facing the flow, the pressure hill at the flat face would be wider than the pressure hill at the convex face of the arc tab facing the flow. Because of this, the size of the vortices formed by the streamlines negotiating these relatively wider and narrower pressure hills would be of different sizes. Thus, the mixing promoting small-scale vortices shed from the edges of the square and arc tabs would be of two different sizes. The difference in the size of the small-scale vortices will cause a noticeable difference in the mixing process caused by these tabs.

From the vortex theory, it can be envisaged that the differential shear at the edge of the free jet, caused by the jet moving at a finite speed with the surrounding still air would result in the formation of vortices at the jet periphery. These vortices are bound to be large-scale structures, in accordance with the theory that the size vortices formed at an edge (free or rigid) will be proportional to the radius curvature of the edge. It is known that the outer edge of the jet may be approximated as a diverging straight line; even though it is not steady[14]. For the uncontrolled jet, i.e. when there is no tab placed at the nozzle exit, the large-scale vortices formed at the jet boundary would entrain mass from the surroundings and carry that to the downstream. In the process, the large-scale vortex, being highly unstable, would break into small-scale structures and carry the entrained mass towards the jet centreline. But this process of mass transport would begin only at a downstream station from the location where the large structure is formed. In other words, it may be stated that the mixing process in the case of an uncontrolled jet will take place only after a time lag between the large-scale vortex formation and its break-up. But the vortices formed at the edges of the tabs, being proportional to the tab half-width, are bound to be small-scale structures. When these small-scale structures are shed right at the nozzle exit, for the jet controlled with tabs, mass entraining large-scale vortices and mass transporting small-scale vortices would prevail right from the nozzle exit. This environment of the existence of large and small vortices right at the nozzle exit might establish an environment that is suitable for faster mixing of the jet with the surroundings. Thus, the controlled jet is expected to enjoy faster mixing than the uncontrolled one. But the level of pressure gradient at the nozzle exit will influence the mixing process. In this work, the efficiency of the mixing promoting vortices shed by the tabs in the pressure of different levels of pressure gradient is studied, both quantitatively and qualitatively. Though promoting mixing, especially in the near field would be of benefit from the stealth capability, base-heating reduction and shock-noise reduction points of view, there is an adverse effect in terms of thrust loss. Since the placement of the tab at the nozzle exit blocks the precious nozzle area, this reduction in exit area would result in a momentum thrust loss, which is not desirable from propulsion point of view. Thus, it is a compromising balance between the advantages in terms of reduced infrared signature, reduced base heating and reduced shock-associated noise and disadvantages such as the thrust loss due to area blockage and the drag caused by the tab itself.

2.3 Instrumentation

Pitot pressure variation along the jet centreline and in the directions along and normal to the tab, at specified axial locations were measured with a 16-channel Pressure Systems 9010 transducer with a range of 0–2.1 MPa. The accuracy of the transducer (after re-zero calibration) is specified to be $\pm 0.15\%$ full scale. This uncertainty range is for the transducer itself. The pressure measurements in the jet flow field was done using a pitot tube of 0.4 mm inner diameter and 0.6 mm outer diameter, mounted on a rigid three-dimensional traverse; with a resolution of 0.1 mm in linear translation. In all measurements, the pitot probe stem was kept normal to the jet axis with its sensing hole facing the flow. The pressure measured is the mean pitot pressure, which is the average of 250 samples per second.

https://doi.org/10.1017/aer.2017.114 Published online by Cambridge University Press

Pressure distribution along the jet centreline was measured from the nozzle exit to 20D, at uniform intervals of 1 mm. In the directions along Y and Z, the pitot pressure distribution was measured from one edge of the jet to the opposite edge, at 1 mm intervals, without assuming any symmetry. In the supersonic region of the jet core, the pitot pressure measured will not be influenced by the disturbances in the downstream stations, since in a supersonic flow no disturbance can propagate upstream. Also, the spread of the jet will not introduce any error to the pitot pressure measured, since the included angle of the jet spread is about 10°[10] and the pitot probe is insensitive to pitch and yaw angles up to about ±11°[16]. The waves prevailing in the supersonic jet core were visualised using a shadowgraph system with a helium spark arc light source in conjunction with a concave mirror. The shadowgraph images were recorded using a still camera.

2.4 Data accuracy

The settling chamber pressure during the experiments of present investigation was maintained within ±2%, for all the NPRs studied. The movement of the pitot probe mounted on the traverse had a resolution of ±0.1 mm in the linear translation. The repeatability of the pressure measurements was within ±3%.

3.0 RESULTS AND DISCUSSION

The measured data consists of the pitot pressure variation along the jet axis (X-direction) and in the directions along the major (Z-direction) and the minor axis (Y-direction) of the elliptical convergent-divergent nozzle of aspect ratio 2. The measured pressures are presented as such, in the non-dimensional form, because calculating Mach number from the measured pressure is impossible for the present field because of the complex wave pattern prevailing in the jet field[14,15]. One of the serious difficulties associated with the analysis of the experimental data of supersonic jets to quantify the core length, characteristic decay and far-field decay is that the measured pitot pressure cannot be deduced to Mach number (or) velocity. This is because, unlike subsonic flow in which the static pressure across the jet is always the surrounding environment pressure because of the correctly expanded state, the supersonic jet is wave dominated in the core region. Because of the presence of compression and expansion waves of varying strength, neither the pitot nor the static pressure is constant across the jet, even at a specific axial location. Furthermore, the waves prevailing in the jet core are complex due to their nonlinear nature. In addition to this, because of the crossing of waves from the edges of periphery from one end to another end, the flow encounters mixed Mach numbers made up of subsonic and supersonic values. Therefore, the use of the isentropic pressure-Mach number relation, normal shock relation, or the Rayleigh pitot formula for calculating the Mach number distribution in the jet flow field is ruled out. Therefore, it is a usual practice to use the measured pitot pressure, which is essentially the total pressure behind the normal shock at the nose of the pitot probe in the non-dimensional form, by dividing with the settling chamber pressure with which the jet is run, to discern the details of the core length, rate of characteristic decay, and the location where the jet becomes fully developed[15].

3.1 Centreline pressure decay (CPD)

The measured pitot pressure distribution along the jet axis of the uncontrolled jet and jets controlled with limiting tabs, of square (flat) and circular arc cross-section, placed along the

https://doi.org/10.1017/aer.2017.114 Published online by Cambridge University Press

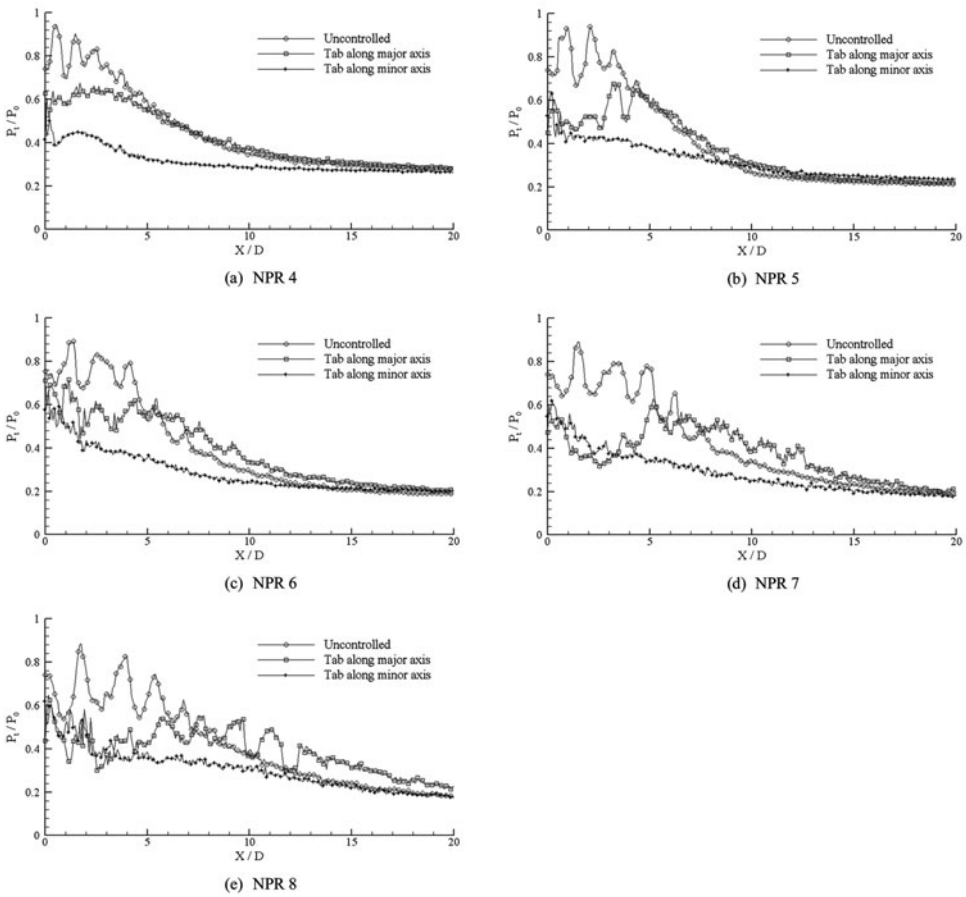


Figure 2. Centerline pressure decay for flat tab.

major and minor axis of the exit plane of the elliptical nozzle of AR4 is presented in Figs 2 and 3. In Figs 2 and 3, the centreline pressure decay of the jet controlled with limiting tab is shown along with its uncontrolled counterpart. Figures 2(a)–2(e), compare the centreline pressure decay for flat limiting tab at nozzle pressure ratios of 4 to 8, respectively, in steps of one. Figure 2(a), gives the centreline pitot pressure variations of the controlled and uncontrolled jets, at NPR 4. NPR 4 for Mach 2 jet is an over-expanded state with an overexpansion level of about 49% ($P_e/P_a = 0.511$). Therefore, at the nozzle exit there will be an oblique shock cone positioned, leading to compression of the over-expanded flow coming out the nozzle to attain equilibrium with the backpressure, namely the atmospheric pressure to which the jet is discharged. The oblique shocks of opposite family from the extremities of the opposite diametric locations of the nozzle exit would be reflected as compression waves from the jet barrel shock. The reflected compression waves would coalesce, forming a shock. The shocks thus formed would travel to the jet centreline and intersect and pass through. The intersecting shocks will travel to the second barrel shock and reflect as expansion rays from the boundary for the barrel shock. This process will continue up to the end of the supersonic core. Core length for supersonic jet is defined as axial distance from the nozzle exit at which characteristic

https://doi.org/10.1017/aer.2017.114 Published online by Cambridge University Press

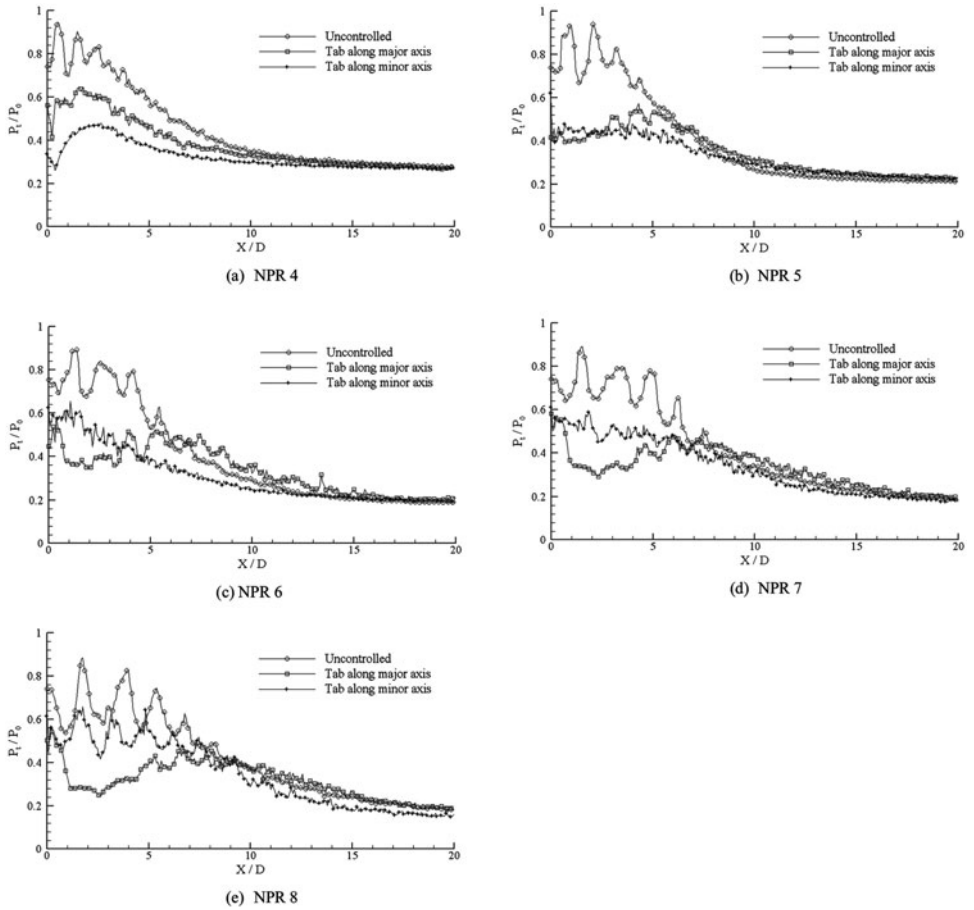


Figure 3. Centerline pressure decay for arc tab.

decay begins. For NPR 4, from Fig. 2(a), it is seen that the core length for the uncontrolled jet is 2.5D. For the flat tab along the minor axis, the core length comes down to 2D. But, for the flat tab along the major axis, the core length extends to 3.5D. This clearly indicates that the tab along the minor axis promotes the mixing, leading to a core length reduction of 20% and the tab along the major axis results in reduced mixing and protects the core to become longer than that of the uncontrolled jet by 40%. This shows that the mixing efficiency of the smaller vortices shed from the tab is influenced by the orientation of the tab. The mixing of the controlled jet in characteristic decay and far field region is more or less similar to that of the uncontrolled jet. The centreline decay of the controlled and uncontrolled jets at NPR 5 are compared in Fig. 2(b). NPR 5 is also an over-expanded state for the jet, but with a reduced level of adverse pressure gradient than NPR 4. At this over-expanded state, limiting flat tab along the minor axis promotes the mixing greatly, leading the jet core to become as short as 0.6D from 4.3D. This amounts to a core length reduction of about 86%. In the far field, the decay of the uncontrolled and controlled jets is almost the same for this NPR also. The core length for tab along major axis is 5.0D, which is 0.7D longer than the uncontrolled jet core. With a further decrease in adverse pressure gradient, corresponding to NPR 6, as seen

https://doi.org/10.1017/aer.2017.114 Published online by Cambridge University Press

in Fig. 2(c), even though the flat tab along the minor axis continues to promote mixing, the mixing caused is found to be inferior to that at NPR 5. The core length for tab along the minor axis is 2.5D, amounting to a reduction of only 63%. At the NPR 6 tab along the major axis also shows a decrease in core length, the decrease is smaller than that for the tab along the minor axis. The core length reduction for tab along major axis is 36%.

In the presence of marginal adverse pressure gradient corresponding to NPR 7, as seen in Fig. 2(d), the flat tab along the minor axis results in a significant decrease in the core length of 84%. For the tab along the major axis, the core length is 5.2D and that for the uncontrolled jet is 7.5D.

For NPR 8, which corresponds to almost correctly expanded state (the isentropic NPR for correct expansion of Mach 2 nozzle is 7.82) or with marginally under-expanded state, as seen from Fig. 2(e), the core length for the uncontrolled jet is 8.2D. Tab along the minor axis reduces the core length to 5.0D from 8.2D, and tab along the major axis shows severe pressure oscillations approximately up to 13D, exhibiting a very long core length and reduced mixing characteristics in comparison to uncontrolled jet. The core length reduction achieved with the limiting flat and arc tabs are calculated for all the NPRs. The reduction in core length can be defined as

$$\text{Reduction in core length} = [(\text{Core})_{\text{uncontrolled jet}} - (\text{Core})_{\text{controlled jet}}]/(\text{Core})_{\text{uncontrolled jet}}$$

On the basis of the above discussion, it can be concluded that, for enhancing the jet mixing, flat tab along the minor axis is better than that along the major axis, at all the levels of the pressure gradients at the nozzle exit, tested in this study. For NPRs 4 and 5, the flat tab along the major axis results in protection of the jet core, resulting in a longer core than the uncontrolled jet. The jet mixing is enhanced when the adverse pressure gradient at the nozzle exit is decreased by changing the NPR from 6 to 7, resulting in a shorter core than the uncontrolled jet. But the mixing enhancement caused is less for the tab along the minor axis. At lower nozzle pressure ratios, the behaviour of the controlled jet in far field is similar to the uncontrolled jet. But in the characteristic decay region, the decay of the controlled jet is faster than the uncontrolled jet. In the presence of zero/marginal favourable pressure gradient, there is a decrease of 39% in core length for tab along the minor axis and a large increase in the core length for the case of tab along the major axis is found.

The centreline pressure decay of the uncontrolled jet and the jet controlled with limiting arc-tab along the major and minor axes are compared in Figs 3(a)–3(e), for all the nozzle pressure ratios of the present study. It is seen in Fig. 3(a) that, at NPR 4, an increased core length is found for both the orientations of tab. For the tab along the minor axis at NPR 4 core length is found to be 2.7D, which amounts to about 8% increase in core length. The tab along the major axis has an increased core length of 3.5D, which is about a 40% increase in core length of the controlled jet compared to the uncontrolled jet.

For NPR 5, as seen from Fig. 3(b), the tab in both the orientations promotes the near field mixing to a large extent. But the enhanced mixing leading to core length reduction caused by the tab along minor axis is only marginal. The core length for the uncontrolled jet is 4.3D and that for the tab along minor axis is 4D. Thus, just a 7.5% reduction in core length is caused by this orientation of the tab at the nozzle exit. For the tab along the major axis, the enhanced mixing causes the waves in the core to become weaker and the core becomes longer than the uncontrolled jet. However, the mixing of the controlled jet in regions beyond the core is found to be better than the uncontrolled jet.

https://doi.org/10.1017/aer.2017.114 Published online by Cambridge University Press

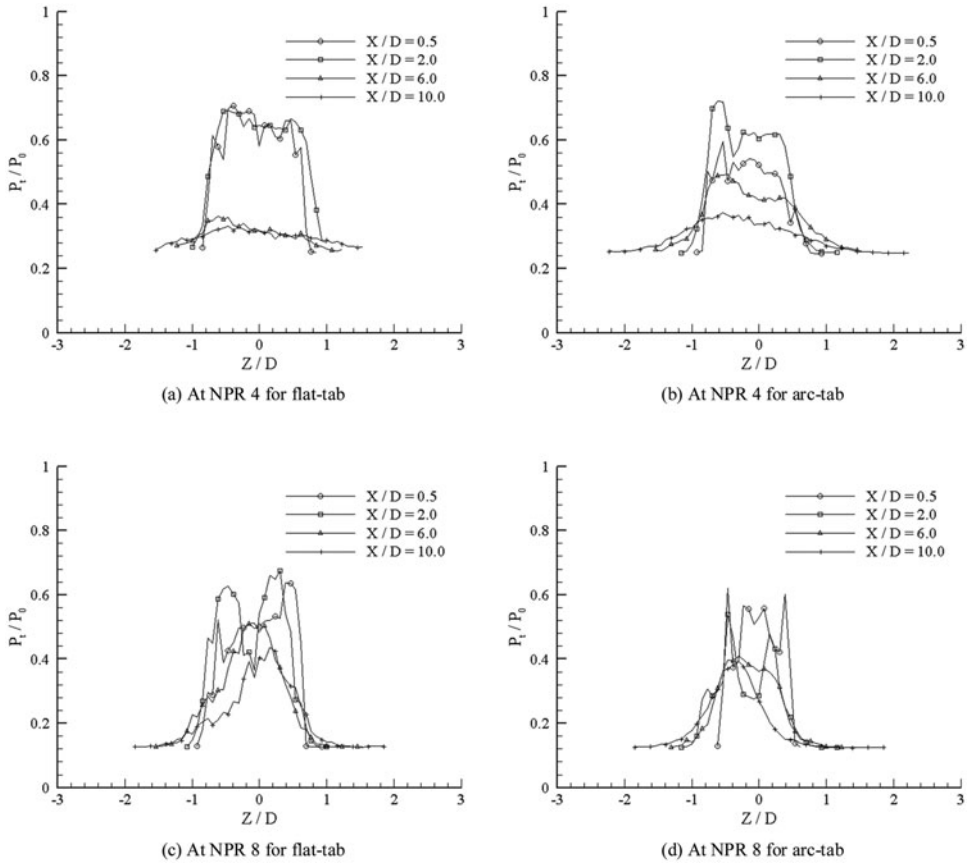


Figure 4. Profile plots for flat and arc tab along major axis.

At NPR 6, as seen in Fig. 3(c), the core lengths for the uncontrolled jet, for tab along the minor and major axes are 6.75D, 3.0D and 7.5D, respectively. Thus, the tab along the minor axis shows a decrease of 55% in the core length, but the tab along the major axis shows extended core length of 7.5D with respect to the uncontrolled jet.

At NPR 7, as seen in Fig. 3(d), the core length for tab along the minor axis is 4.7D and core length of 7.4D is found for tab along major axis. Core length obtained from centreline pressure decay plot shows that decrease of about 37% in core length is obtained for tab along minor axis and for tab along major axis, core length is found to be almost similar to uncontrolled jet.

For NPR 8, as seen in Fig. 3(e), the core length for uncontrolled jet is 8.2D which is more or less equal to core length for tab along major axis. Further, a decreased core length of 7.5D is found for tab along minor axis, which corresponds to reduction of 8.5% in core length.

Based on the above results, it is evident that, for both geometries of the tab, the tab along the minor axis enhances mixing for most cases in range of tested NPRs. At higher overexpansion levels as well as at marginal under-expansion levels for both the geometries, tab along the major axis results in increased core length than uncontrolled one. For all the levels of overexpansion, the mixing for the controlled jet is found to be better than that of the uncontrolled jet, in characteristic decay region. The best mixing caused by the flat tab along the minor axis is at NPR 5, resulting in a core length reduction of 86%.

https://doi.org/10.1017/aer.2017.114 Published online by Cambridge University Press

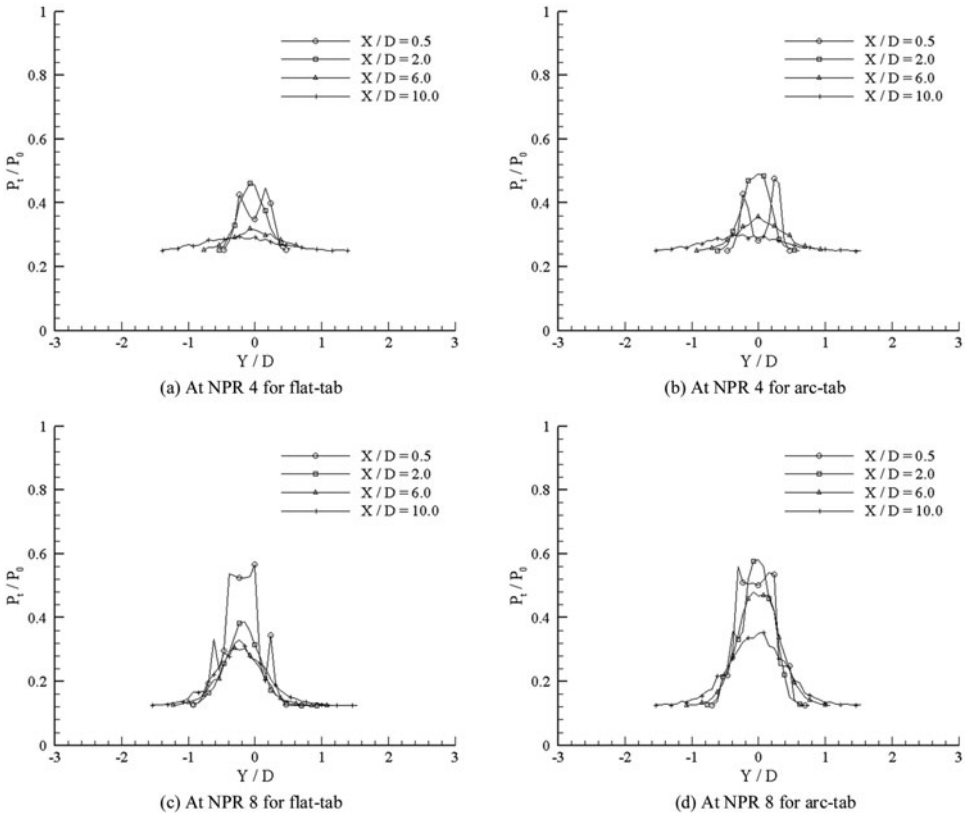


Figure 5. Profile plots for flat and arc tab along minor axis.

3.2 Pressure profile

The pitot pressure (P_t) distribution, measured along the major and minor axes directions of the controlled jets, is non-dimensionalised by dividing with the settling chamber pressure P_0. The distance in direction of major axis (Z-direction) and minor axis (Y-direction) are made non-dimensional by dividing them with nozzle exit diameter (D).

In Figs 4(a)–4(d), the pressure profiles for the flat and arc tabs along the major axis (Z-direction), at different NPRs are presented. At NPR 4, as seen in Fig. 4(a), in near field, at $X/D = 0.5$, the pressure increases steeply to around 0.72 up to $Z/D = -0.5$, and then shows erratic behaviour up to $Z/D = 0.5$. At $Z/D = 0.0$, the value of P_t/P_0 is around 0.6 which implies that the velocity of jet is maximum at the centre. At $X/D = 2.0$, more or less the same trend is followed by the pressure profile as in case of pressure profile at $X/D = 0.5$.

Both of these locations are within the core region of jet. At $X/D = 6.0$ which is in characteristic decay region, the larger spread of the pressure profiles implies faster mixing. Finally, at $X/D = 10.0$, the jet has encountered the characteristic decay and the pitot pressure decay shows almost fully developed nature. In Fig. 4(b), at $X/D = 0.5$, pressure P_t/P_0 first increases up to a value of around 0.6 and then drops to a value of less than 0.5 up to $Z/D = -0.5$, which means that maximum velocity is attained to the left of $Z/D = 0.0$, due to which figure loses its symmetry. An almost similar trend is followed for $X/D = 2.0$ as

https://doi.org/10.1017/aer.2017.114 Published online by Cambridge University Press

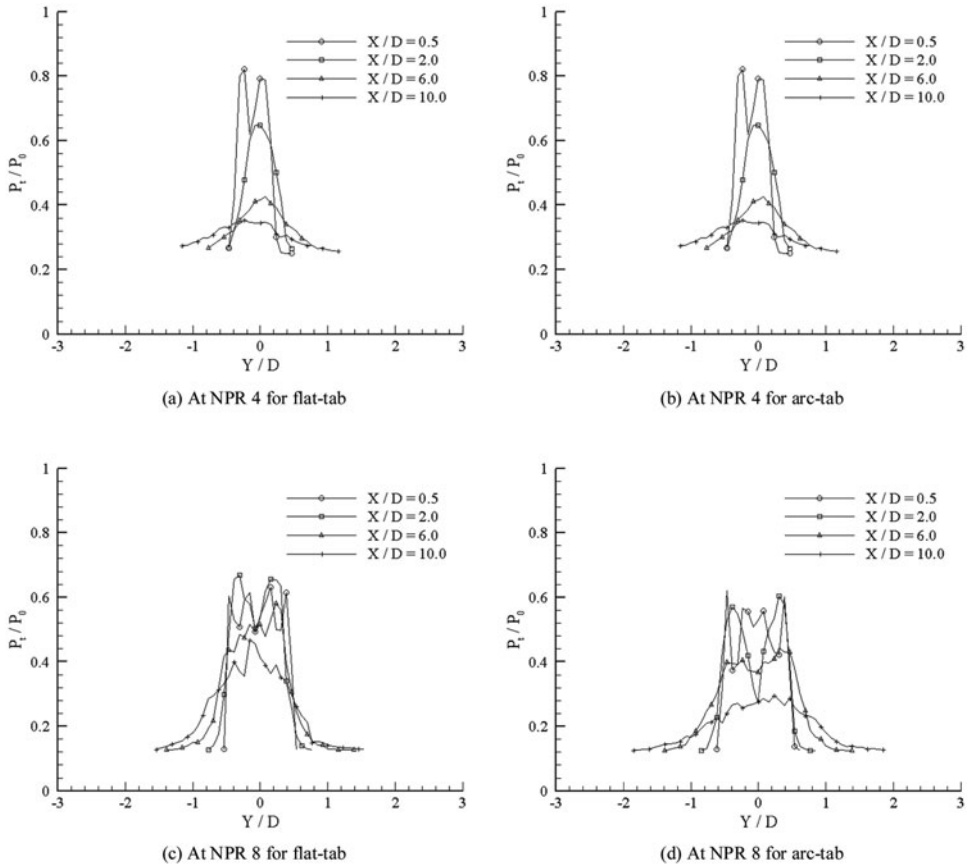


Figure 6. Profile plots for flat and arc tab along major axis.

for X/D = 0.5, except that peak pressure attained is around 0.73. For X/D = 6.0, the peak pressure is much higher than that of the limiting flat tab at X/D = 6.0, which shows that flat tab is more effective in mixing promotion.

In Fig. 4(c) (at NPR 8), for flat tab the pressure profiles are full of pressure oscillations and peak pressure attained by the pressure profile in near-field is less than maximum value attained at lower NPRs in the previous figures. At X/D = 0.5, minimum pressure is attained at around Z/D = 0.0. In Fig. 4(d), because arc tab pressure profiles are having fewer oscillations and are in characteristic decay region, pressure profiles are quite orderly in comparison to those for flat tab at this NPR. The jet spread in far field for arc-tab is more compared to that of flat tab for almost all locations.

The profile plots in Y-direction for flat and arc tabs along minor axis at different X/D locations are shown in Figs 5(a)–5(d). In Fig. 5(a), at this lowest NPR pressure profiles are quite orderly and symmetric than they were in the case of Fig. 4. The peak pressure attained at X/D = 2.0 is around $P_t/P_0 = 0.5$, which is lower than that for the case of tab along major axis at this X/D location in Fig. 4(a).

For X/D = 2.0, at the centre (Y/D = 0.0) there is minimum pressure and hence maximum velocity is attained at this point. The jet spread in far field is from Y/D = −1.5 to +1.5.

https://doi.org/10.1017/aer.2017.114 Published online by Cambridge University Press

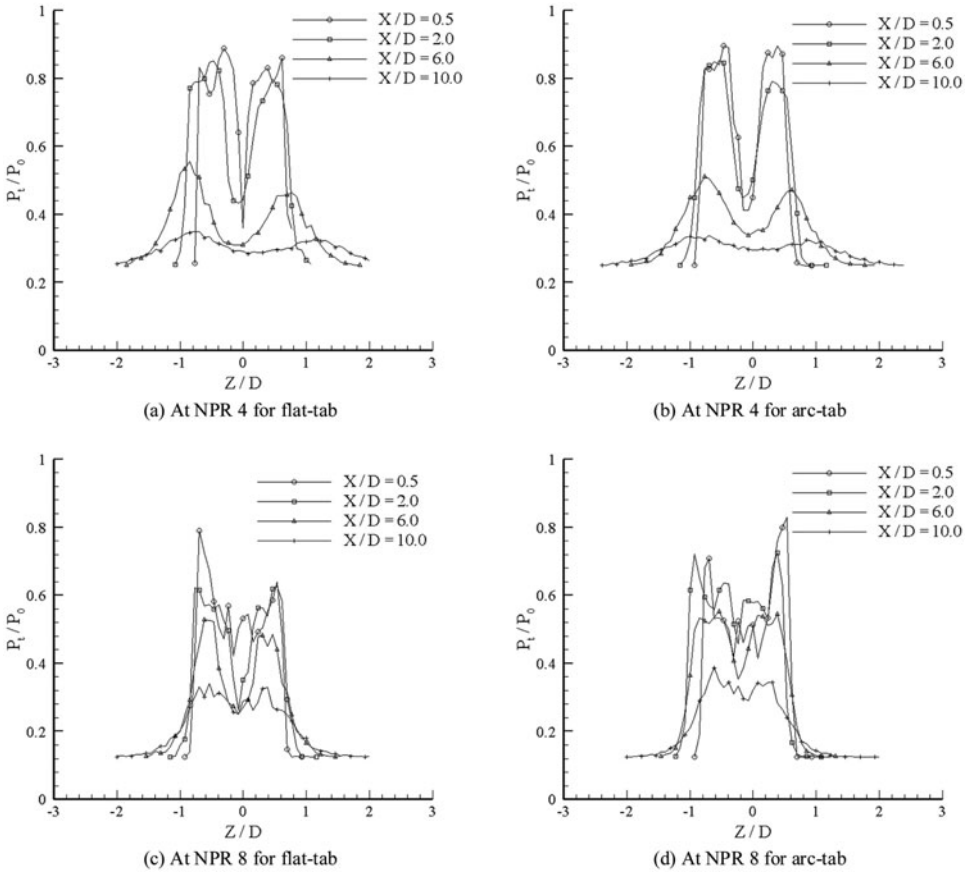


Figure 7. Profile plots for flat and arc tab along minor axis.

Profiles are symmetric along the centre. The arc-tab along minor axis at NPR 4 shows similar behaviour as flat tab, except for $X/D = 2.0$ at the centre ($Y/D = 0.0$), a minimum value of P_t/P_0 around 0.25 is obtained. From Figs 5(c) and 5(d), it can be said that, as NPR increases, the pressure oscillations start becoming evident in pressure profiles and thereby destroys its symmetry as well as its orderly pattern. With the increase in NPR, the behaviour in characteristic decay region starts degrading and becomes full of pressure oscillations while at lower NPR this region is quite smooth and clean in terms of pressure oscillations. The jet spread in far field also decreases with increase in NPR. These inferences are independent of the fact that whether tab is along major or minor axis or it is flat or arc tab. The above features in pressure profiles show that in general with the increase in NPR the effectiveness of tab decreases. Performance of flat or arc tab along minor axis is better than the same tab along major axis.

In Figs 6(a)–(d), the pressure profiles in the Y direction for flat and arc tab along major axis (Z direction) are compared. In Fig. 6(a), at NPR 4 value of P_t/P_0 attains a value greater than 0.8. At $X/D = 2.0$, the velocity at the centre is minimum and profile is symmetric along $Z/D = 0.0$. In the characteristic decay region, spread is less in comparison to spread in Z direction as shown in Fig. 4, for same orientation of tab. For Fig. 6(b) in near field at

https://doi.org/10.1017/aer.2017.114 Published online by Cambridge University Press

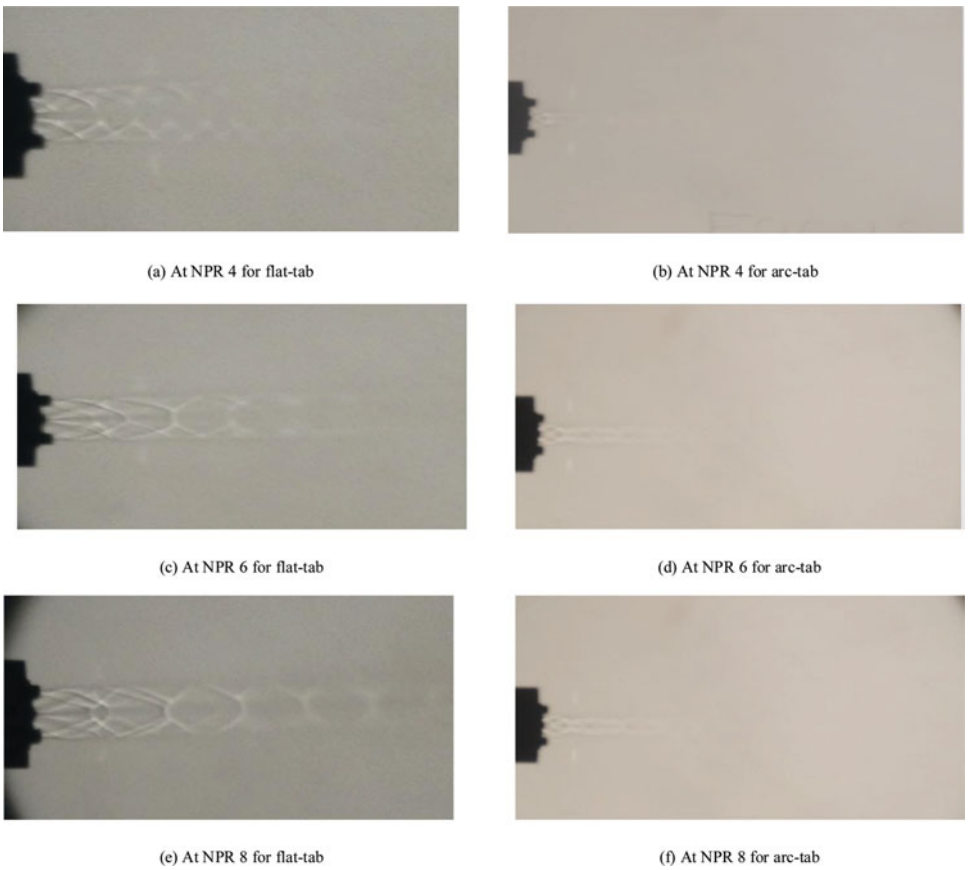


Figure 8. (Colour online) Shadowgraph pictures for flat and arc tabs along major axis.

$X/D = 0.5$, the maximum value of pressure ratio P_t/P_0 is less than the case of flat tab. In the characteristic decay region, almost the same pattern is followed as in case of flat tab except that the spread is more in the case of arc tab. Finally, at NPR 8 in Figs 6(c) and 6(d), which is an under-expanded level, the pressure profiles lose their symmetry and show severe pressure oscillations. The peak pressure attained in near field at NPR 8 is less than that in case of NPR 4 for flat tab in Fig. 6(a) and lowest value of P_t/P_0 is attained at NPR 8 for arc-tab in Fig. 6(d), in near field.

In Figs 7(a)–(d), the pressure profiles in Z direction for flat and arc tab along minor axis (Y-direction) are compared. In Fig. 7(a), the pressure hike in near field is close to $P_t/P_0 = 0.85$. In the far field, the spread is greater than the profiles shown in Fig. 6, where tab was along major axis. Pressure profiles in near field are quite symmetric and attain minimum pressure at $Z/D = 0.0$. For the case of arc tab at NPR 4 in Figure 7(b), the maximum pressure attained in near field is comparable to the case at NPR 4 for flat tab in Figure 7(a) and in far field the spread is found to be tremendous. The spread in far field for cases of tab along minor axis ensures its effective performance over tab along major axis. In Figs 7(c) and 7(d), the same behaviour is repeated as for the other profile plots, which is that the maximum pressure attained in near field decreases and the spread in far field decreases, in totality a decrease in mixing performance is obtained.

https://doi.org/10.1017/aer.2017.114 Published online by Cambridge University Press

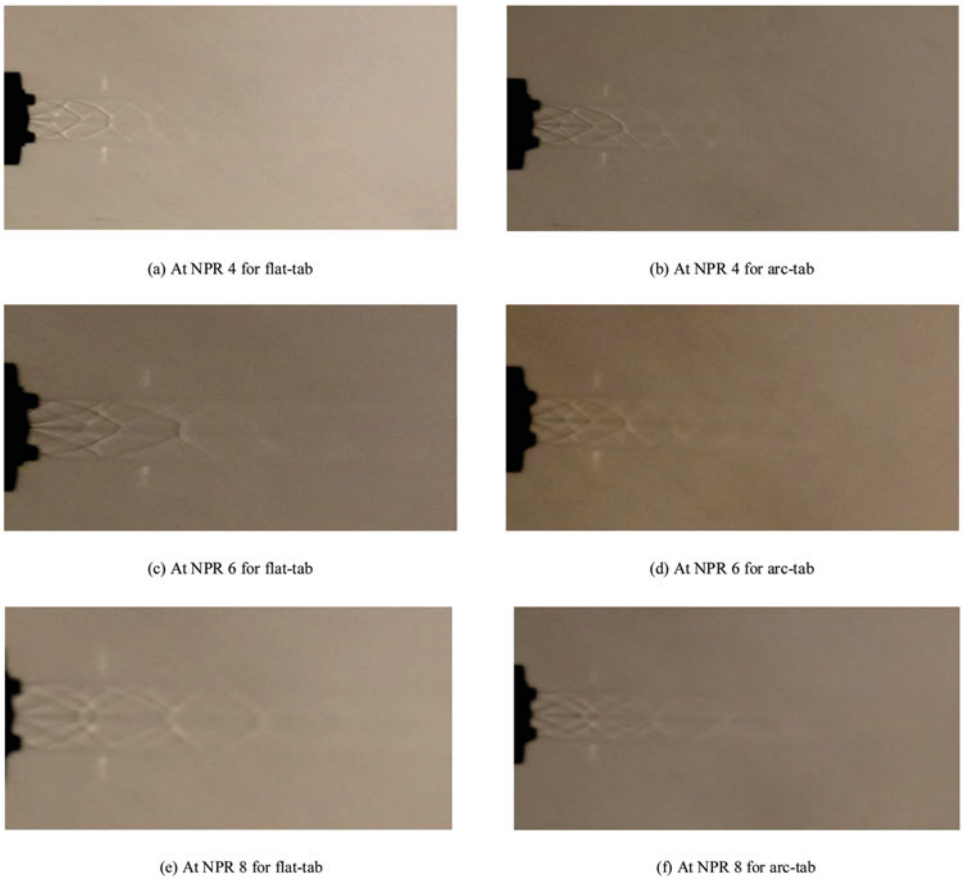


Figure 9. (Colour online) Shadowgraph pictures for flat and arc tabs along minor axis.

3.3 Visualisation

Shadowgraph pictures of the elliptical jet of aspect ratio 2:1, with limiting flat and arc tabs fixed along different orientations are shown in Figs 8 and 9. For controlled jets, visualisation has been carried out viewing along and normal to the tabs but in Figs 8 and 9, the shadowgraph pictures presented are along the tab. In Fig. 8(a), for flat tab along major axis, at NPR 4, which is an over-expanded state for the Mach 2 nozzle, the oblique shocks at the nozzle exit are clearly seen. These oblique shocks cross each other at the jet axis and reach the barrel shock. On reaching barrel shock, the oblique shock reflects as expansion fan, because reflection from fluid boundary is unlike[14]. This kind of wave reflection continues to some downstream distance. The distance between successive shock reflection points (kinks) is called the shock cell length. At this low nozzle pressure ratio of 4, the jet seems to be bifurcated due to the presence of the limiting tab and shock cells are weaker by nature. Contrary to this, in Fig. 8(b), for arc tab, the width of the shock cell structure is found to be very thin and individual shock cells are not visible. In Figs 8(c) and 8(e), for the case of flat tab, the number of shock cell increases and hence mixing due to tab decreases, especially at nozzle pressure ratio of 8 (at marginally under-expanded state) jet boundary gets widened and 5 shock cells are visible,

https://doi.org/10.1017/aer.2017.114 Published online by Cambridge University Press

among which the initial two are quite prominent and the rest are feeble. For the arc tab in Figs 8(d) and 8(f), shock structure starts becoming evident but still wave dominance is confined to a very thin region.

In Figs 9(a)–(f), the shadowgraph pictures for the jets controlled with the flat and arc tabs along minor axis are presented. As we know from the centreline decay pressure plots, flat tab along minor axis is a better mixing promoter than the same along major axis. The shadowgraph pictures for NPR4, shown in Figs 9(a) and 9(b) show that the spread of the waves in the core of the jet controlled with flat tab is larger than that of arc tab. Also, for the flat tab jet is divided into two parts, whereas this is does not happen for the arc tab. The number of shock cells increase and the jet boundary seems to be wider with increase in nozzle pressure ratio regardless of orientation or geometry of tab.

4.0 CONCLUSIONS

The results of the present study demonstrate that it is not just the orientation of the tab but the orientation, tab geometry and level of pressure gradient at the nozzle exit playing a dominant role in dictating the mixing promotion caused by the tabs of two different geometry. The mixing promotion caused by the tab along minor axis is found to be appreciably greater than that along the major axis. The maximum core length reduction caused by the flat tab along the minor axis is 86% at NPR 5. Moreover, with the arc tab along major axis, the core is always protected, for the range of nozzle pressure ratios tested. Overall performance of flat limiting tab is found to be superior in comparison to arc limiting tab.

ACKNOWLEDGEMENTS

The authors would like to thank S M Aravindh Kumar, Ph.D Scholar, High-Speed Lab, Aerospace Engineering, IIT Kanpur, for giving the data for Mach 2 elliptical jet (uncontrolled) used for comparison in this article.

REFERENCES

1. HUSAIN, H.S. and HUSSAIN, A.K.M.F. Controlled excitation of elliptical jets, *Physics of Fluids*, 1983, **26**, pp 2763-2766.
2. HO, C.M. and GUTMARK, E.J. Vortex induction and mass entrainment in a small-aspect ratio elliptical jet, *J. Fluid Mechanics*, 1987, **179**, pp 383-405.
3. GUTMARK, E.J., SCHADOW, K.C. and WILSON, K.J. Noncircular jet dynamics in supersonic combustion, *J. Propulsion and Power*, 1989, **5**, pp 529-533.
4. GUTMARK, E.J., SCHADOW, K.C. and WILSON, K.J. Subsonic and supersonic combustion using noncircular injectors, *J. Propulsion and Power*, 1991, **7**, pp 240-249.
5. BRADBURY, L.J.S. and KHADEM, A.H. The distortion of a jet by tabs, *J. Fluid Mechanics*, 1995, **70**, (4), pp 801-813.
6. SAMIMY, M., ZAMAN, K.B.M.Q. and REEDER, M. F. Effect of tabs on the flow and noise field of an axisymmetric jet, *AIAA*, 1993, **31**, pp 609-619.
7. RATHAKRISHNAN, E. Experimental studies on the limiting tab, *AIAA*, 2009, **47**, pp 2475-2485.
8. ARUN KUMAR, P. and RATHAKRISHNAN, E. Corrugated triangular tabs for supersonic jet control, *Proceedings of the Institution of Mech. Engineers, Part G: J. Aerospace Engineering*, 2014, **228**, pp 831-845.
9. AHUJA, K.K. Mixing enhancement and jet noise reduction through tabs plus ejectors, AIAA Paper No. 93-4347, 25-27 October 1993, Monterey, CA.

https://doi.org/10.1017/aer.2017.114 Published online by Cambridge University Press

10. Arun Kumar, P. and Rathakrishnan, E. Triangular tabs for supersonic jet mixing enhancement, *The Aeronautical J*, 2014, **118**, (1209), pp 1245-1278.
11. Bohl, D. and Foss, J.F. Characteristic of the velocity and streamwise vorticity fields in a developing tabbed jet, AIAA Paper No. 95-0102, 9-12 January 1995.
12. Ahuja, K.K. and Brown, W.H. Shear flow control by mechanical tabs, AIAA Paper No. 89-0994, 1989.
13. Aravindh Kumar, S.M. and Rathakrishnan, E. Characteristics of a supersonic elliptical jet, *The Aeronautical J*, 2016, **120**, pp 495-519.
14. Rathakrishnan, E. *Applied Gas Dynamics*, 2010, Wiley, Hoboken, New Jersey, US.
15. Aravindh Kumar, S.M. and Rathakrishnan, E. Characteristics of controlled Mach 2 elliptical jet, *J Propulsion and Power*, 2015, **32**, pp 121-133.
16. Rathakrishnan, E. *Instrumentation, Measurements and Experiments in Fluids*, 2nd ed., 2017, CRC Press, Boca Raton, Florida, US.

https://doi.org/10.1017/aer.2017.114 Published online by Cambridge University Press